HHS Public Access

Author manuscript

Cancer Res. Author manuscript; available in PMC 2017 May 01.

Published in final edited form as:

Cancer Res. 2016 May 1; 76(9): 2824–2835. doi:10.1158/0008-5472.CAN-15-3010.

Analysis of liver tumor-prone mouse models of the Hippo kinase scaffold proteins RASSF1A and SAV1

Xiaoying Zhang[2,6], **Cai Guo**[2,7], **Xiwei Wu**[3], **Arthur X. Li**[3], **Limin Liu**[2,8], **Walter Tsark**[4], **Reinhard Dammann**[5], **Hui Shen**[1], **Steven L. Vonderfecht**[4], and **Gerd P. Pfeifer**[1,2,*]

[1]Center for Epigenetics, Van Andel Research Institute, Grand Rapids, MI, USA

[2]Department of Biology, Beckman Research Institute, City of Hope, Duarte, CA

[3]Department of Molecular and Cellular Biology, Beckman Research Institute, City of Hope, Duarte, CA

[4]Division of Comparative Medicine, Beckman Research Institute, City of Hope, Duarte, CA

[5]Institute for Genetics, Justus-Liebig-University, Giessen, Germany.

Abstract

The tumor suppressor gene RASSF1A is epigenetically silenced in most human cancers. As a binding partner of the kinases MST1 and MST2, the mammalian orthologues of the Drosophila Hippo kinase, RASSF1A is a potential regulator of the Hippo tumor suppressor pathway. RASSF1A shares these properties with the scaffold protein SAV1. The role of this pathway in human cancer has remained enigmatic inasmuch as Hippo pathway components are rarely mutated in tumors. Here we show that Rassf1a homozygous knockout mice develop liver tumors. However, heterozygous deletion of Sav1 or co-deletion of Rassf1a and Sav1 produced liver tumors with much higher efficiency than single deletion of Rassf1a. Analysis of RASSF1A binding partners by mass spectrometry identified the Hippo kinases MST1, MST2 and the oncogenic IkB kinase TBK1 as the most enriched RASSF1A-interacting proteins. The transcriptome of Rassf1a−/− livers was more deregulated than that of Sav1+/− livers, and the transcriptome of Rassf1a−/−, Sav1+/− livers was similar to that of Rassf1a−/− mice. We found that the levels of TBK1 protein were substantially upregulated in livers lacking Rassf1a. Furthermore, transcripts of several beta tubulin isoforms were increased in the Rassf1a-deficient livers presumably reflecting a role of RASSF1A as a microtubule-stabilizing protein. In human liver cancer, RASSF1A frequently undergoes methylation at the promoter but this was not observed for MST1, MST2, or SAV1. Our results suggest a multifactorial role of RASSF1A in suppression of liver carcinogenesis.

*Correspondence: Gerd P. Pfeifer, PhD, Center for Epigenetics, Van Andel Research Institute, 333 Bostwick Ave. NE, Grand Rapids, MI 49503, ; Email: gerd.pfeifer@vai.org, 616-234-5398.

[6]Present address: Department of Pediatrics, Univ. of Tennessee Health Science Center, Memphis, TN.

[7]Present address: Department of Biology; California Institute of Technology, Pasadena, CA.

[8]Present address: Department of Biochemistry and Molecular Genetics, Univ. of Virginia, Charlottesville, VA.

The authors disclose no potential conflicts of interest.

Introduction

Liver cancer is one of the leading causes of cancer death worldwide. The Ras association domain family 1 (*RASSF1*) gene is located at chromosome 3p21.3 in a region frequently deleted in human solid tumors. The *RASSF1* locus encodes two major transcripts referred to as *RASSF1A* and *RASSF1C*, which code for two proteins differing in their N-termini (1). The *RASSF1A* transcript and protein are frequently absent from human tumors due to methylation of the *RASSF1A* isoform-specific promoter (1,2). Methylation of the *RASSF1A* promoter often occurs at an early stage of tumor progression (3). Mice with *Rassf1a* gene deletion are prone to carcinogen-induced and spontaneous tumorigenesis (4-6).

Although RASSF1A encodes a Ras association domain, this protein is effectively recruited to activated Ras only through heterodimerization with its closest homologue NORE1A/RASSF5 (7). RASSF1A is a potent microtubule binding and stabilizing protein (8,9). The non-catalytic protein RASSF1A is found in a complex with the kinases MST1 and MST2, the mammalian orhtologues of the tumor-suppressive *Drosophila* Hippo kinase and is associated with several other proteins of the Hippo pathway (10,11). RASSF1A inhibits the dephosphorylation of MST1/MST2 by phosphatases thus promoting an activated state of MST1/MST2 (12). The core components of the Hippo pathway are highly conserved across species. In mammals, the kinases MST1/MST2 can form a complex with another adaptor protein, SAV1, the mammalian counterpart of the *Drosophila* protein Salvador (13). MST1/MST2 kinases activate two downstream kinases, LATS1 and LATS2 (14). The best-studied effector of the LATS kinases is YAP, an oncogenic transcriptional co-activator (15). Phosphorylated YAP is retained in the cytoplasm, which prevents it from activating transcription (16). In this model, the Hippo kinases are negative regulators of YAP. Hippo signaling is an important pathway for inhibition of cancer development in the mouse liver. Liver-specific deletion of *Mst1* and *Mst2* combined, or deletion of *Sav1* alone leads to liver enlargement and effective induction of hepatocellular carcinomas (HCC) or mixed liver tumors in mice [HCC/cholangiocarcinomas (CC)] (17-20).

However, recent genome sequencing of human HCCs has failed to uncover mutations in components of the Hippo pathway (e.g. *MST1/2*, *LATS1/2*, *SAV1*) (21-23). Although amplification and/or overexpression of *YAP* as well as diminished YAP phosphorylation has been seen in a fraction of human liver cancers (19,24,25), the overall impact of this pathway on human cancer is still unclear.

Our current report addresses the role of *Rassf1a* deletion on liver physiology and malignant transformation in the mouse. For comparison, we analyzed mice with single homozygous deletion of *Rassf1a* or heterozygous deletion of *Sav1*, and also created a $Sav1^{+/-}$ $Rassf1a^{-/-}$ double knockout mouse model to study the function of these genes in liver tumorigenesis.

Materials and Methods

Generation of single and double Rassf1a and Sav1 gene knockout mice, tumor studies and liver tissue collection

Rassf1a$^{-/-}$ mice were derived previously (4). We created *Sav1* mutant mice by using standard gene targeting methods to delete exons 1 and 2 in 129S1 mouse embryonic stem cells. Homozygous *Sav1* knockouts died *in utero* as reported previously (26). The *Sav1* knockout colony was maintained in the heterozygous state. The *Rassf1a* and *Sav1* mutant mice were crossed to Cre-Deleter/129 mice (27) to remove the neomycin selection cassette. Typical genotyping results are shown in Figure S1. The *Sav1* and *Rassf1a* mutant mice were maintained on the 129S1 background. Four mouse cohorts, Rassf1a$^{+/+}$ *Sav1*$^{+/+}$ (wildtype), *Rassf1a*$^{-/-}$ *Sav1*$^{+/+}$, *Rassf1a*$^{+/+}$ *Sav1*$^{+/-}$, and *Rassf1a*$^{-/-}$ *Sav1*$^{+/-}$, were established and monitored for spontaneous tumor formation, morbidity or death. Mice were euthanized when visibly moribund or whenever a growth/tumor became manifest, and a complete necroscopy was performed. Normal appearing liver or tumor tissues were fixed in 10% neutral-buffered formalin, and the remaining parts of liver tumor tissue and adjacent normal tissue were instantly frozen in liquid nitrogen and then stored at −80°C. The formalin fixed tissues were embedded in paraffin, and then stained with hematoxylin and eosin (H&E).

Western blot and immunoprecipitation analysis

Frozen tissue was ground in liquid nitrogen by using a pestle, and the total proteins were extracted with extraction buffer (50 mM HEPES, pH 7.4, 137 mM NaCl, 10% glycerol, 0.1% Triton-X 100, and 1x complete protease inhibitor cocktail (Roche)). Alternatively, soluble cytosolic fractions were prepared following a published procedure (28). Protein samples were resolved on 12% SDS-polyacrylamide gels and transferred onto nitrocellulose membranes (Bio-Rad). Nitrocellulose membranes were blocked with 5% nonfat milk (Bio-Rad) in PBST (PBS with 0.1% Tween 20) and sequentially incubated with primary antibodies and HRP-conjugated secondary antibodies (Jackson ImmunoResearch Laboratories; West Grove, PA) in 5% nonfat milk in PBST. After incubation, blots were washed three times with PBST. We visualized the immunoreactive bands with Amersham ECL Prime Western Blotting Detection Reagent following the manufacturer's instructions. Immunoprecipitation was performed as described previously (12).

Combined bisulfite restriction analysis (COBRA)

Human liver cancer specimens and adjacent normal liver tissue were obtained from the City of Hope frozen tumor bank on an institutionally approved protocol. Tumor-free liver DNA from accident victims was obtained from Biochain. Genomic DNA was isolated from frozen tissue using the DNeasy Blood & Tissue Kit (Qiagen). One microgram of genomic DNA was treated with sodium bisulfite and the samples were subjected to ‘combined bisulfite restriction analysis’ (COBRA) (29) using primers as described previously (30). PCR products were digested with BstUI or TaqI restriction enzymes (New England Biolabs). These enzymes only cut initially methylated DNA after bisulfite conversion and PCR. The digested PCR products were separated by electrophoresis on 2% agarose gels.

Antibodies

Antibodies against phospho-IkB alpha (Ser32) (catalogue #2859), MST1 (#3682), YAP (#4912), phospho-YAP (Ser127) (#4911), TBK1 (#3013), NFkB1 (#13586), and phospho-p65 (Ser536) (#3033) were purchased from Cell Signaling Technologies. Antibodies against YAP1 (sc-15407), TAZ (sc-48805), SAV1 (sc-135394), and NFkB/p65 (ac-109X) were purchased from Santa Cruz Biotechnology. Lamin B1 (ab16048), TUBB2A (#ab170931) and IkB alpha (ab32518) antibodies were obtained from Abcam. Anti- β-actin (A5441) and anti-FLAG (F7425) antibodies were from Sigma. Anti-MST2 (#1943-1) was from Epitomics, and anti-GAPDH (627408) was from Genetex. Anti-RASSF1A antibodies (M3-04 and M5-06) were raised against the N-terminal exon of RASSF1A (10).

RNA isolation, microarray analysis and cDNA reverse transcription

For total RNA isolation, we followed the instruction of the Ambion Purelink RNA mini kit. cDNA was synthesized from RNA template by using SuperScript III reverse transcriptase (Invitrogen). Real-time PCR amplifications were performed in 96-well optical reaction plates with SYBR Green by using Taq DNA polymerase (Qiagen). We used Affymetrix Gene 1.0-ST microarrays for gene expression analysis of mouse liver RNAs. Microarray data were analyzed using the Bioconductor package “ArrayTools”. Differentially expressed genes were selected by using a cutoff of P <= 0.005 and fold change >= 1.5. Heat maps were created by using Cluster v3.0 and visualized by Java Treeview. Raw data was deposited into the GEO database (accession number GSE73911).

TCGA data analysis

DNA methylation data packages (Version 13) for the TCGA Liver Hepatocellular Carcinoma (LIHC) project were downloaded from the TCGA data portal on Dec 22, 2015. The R package *Homo.sapiens* was used to obtain the genomic locations of each gene, and *GenomicRanges* was used to get DNA methylation probes interrogating +/−1500 bp of the genomic range of the target gene. For each heatmap, the probes (rows) are arranged by their genomic location, and samples are clustered with hierarchical clustering to reveal patterns. Normalized isoform-level RNAseq data were downloaded from Firehose (http://gdac.broadinstitute.org). We used uc003dae for *RASSF1A* and uc003dab for *RASSF1C* expression levels, and for other genes only expressed isoforms were used. Corresponding Log2-transformed gene expression levels are plotted on top of each sample with a relative scale.

Results

Tumor susceptibility of Rassf1a and Sav1 knockout mice

Previous reports suggested that both RASSF1A and SAV1 form a complex through their C-terminal SARAH domains with the Hippo kinases MST1 and MST2 (10,11). To study the contribution of these proteins to tumorigenesis, we generated mouse strains with germ line (whole body) deletion of Rassf1a (*Rassf1a* isoform-specific knockout by deletion of exon 1) and/or *Sav1*. *Rassf1a* homozygous gene knockout mice are viable and fertile (4,5), but, for the Sav1 gene knockout, only heterozygous mice could be obtained. This is due to

embryonic lethality of complete *Sav1* deletion in mice as also reported previously (26). *Rassf1a*$^{-/-}$ *Sav1*$^{+/-}$ mice were viable and fertile. Mouse colonies of four different genotypes, *Rassf1a*$^{+/+}$ *Sav1*$^{+/+}$, *Rassf1a*$^{-/-}$ *Sav1*$^{+/+}$, *Rassf1a*$^{+/+}$ *Sav1*$^{+/-}$, and *Rassf1a*$^{-/-}$ *Sav1*$^{+/-}$, were established on the 129S1 genetic background and were observed for signs of tumor formation over extended periods of time. Overall survival was significantly different between wildtype and *Rassf1a*$^{-/-}$ *Sav1*$^{+/-}$ mice (P= 0.0063; log-rank test) and between *Rassf1a*$^{-/-}$ *Sav1*$^{+/+}$ and *Rassf1a*$^{-/-}$ *Sav1*$^{+/-}$ mice (P<0.001) but not between wildtype and *Rassf1a*$^{-/-}$ *Sav1*$^{+/+}$ (P=0.1016), wildtype and *Rassf1a*$^{+/+}$ *Sav1*$^{+/-}$ (P=0.1144), or between *Rassf1a*$^{+/+}$ *Sav1*$^{+/-}$ and *Rassf1a*$^{-/-}$ *Sav1*$^{+/-}$ (P=0.287) (Fig. 1). Curiously, some *Rassf1a*$^{-/-}$ *Sav1*$^{+/+}$ mice survived to very old age.

Liver tumors developed in 19 of the 45 mice (42%) of the *Rassf1a*$^{-/-}$ *Sav1*$^{+/+}$ genotype (Table 1). These varied from small, solitary nodules to large, multinodular masses that occupied entire lobes of the liver. The tumors were designated as hepatocellular adenomas (HA), hepatocellular carcinomas (HCC), mixed hepatocellular adenomas (mHA), or mixed hepatocellular carcinomas (mHCC) (Table 1). Microscopic features of HA and HCC were typical for these types of tumors (e.g., Fig. S2) and diagnoses were based upon standard histopathologic criteria (31). Tumors designated as mHA or mHCC were morphologically distinct and did not clearly fit into any recognized classification of hepatocellular tumors. They are likely similar to tumors described in *WW45*$^{+/-}$ (same as *Sav1*$^{+/-}$) mice and designated as “mixed-type” liver tumors thought to arise from hepatic progenitor (oval) cells (17). The mHA and mHCC had a component with obvious hepatocellular morphology and a significant second component of cells with small, oval to occasionally round or elongated nuclei and indistinct cytoplasm. These “small cells” formed solid sheets or irregular bands that penetrated into and sometimes surrounded nodules of neoplastic hepatocytes. The nuclei of the cells were occasionally arranged in rows or formed small, duct-like structures (Fig. 2). Because this second cellular component was uniformly small, highly homogeneous, and lacked mitotic figures, the designation of mHA or mHCC was based solely upon the morphology of the hepatocellular component of the tumor. In comparison to the *Rassf1a*$^{-/-}$ *Sav1*$^{+/+}$ mice, only 6 of 30 (20%) wildtype mice had hepatocellular tumors (including one microscopic tumor) and these were all hepatocellular adenomas (Table 1) indicating increased tumor susceptibility and tumor progression in *Rassf1a*-deleted mice (P = 0.046; Chi square test). For the *Sav1*-targeted mice, 47 out of 49 (96%) *Rassf1a*$^{+/+}$ *Sav1*$^{+/-}$ mice were found with liver tumors at ages greater than one year. Similarly, 35 of 39 *Rassf1a*$^{-/-}$ *Sav1*$^{+/-}$ mice (90%) developed liver tumors suggesting that loss of one copy of *Sav1* is a much more potent driver of liver tumor formation than loss of both copies of *Rassf1a* making it likely that loss of *Sav1* is the dominant event in driving tumorigenesis in the double knockout mice (Table 1). Most of the livers from *Sav1*$^{+/-}$ mice showed signs of oval cell hyperplasia (Fig. 2E; Fig. S3). This change was only occasionally observed in *Rassf1a*$^{-/-}$ *Sav1*$^{+/+}$ mice and was not seen in wild type mice. Oval cells are considered bipotential progenitors capable of differentiating into hepatocytes or cholangiocytes. However, distinct features of CC, e.g., clear gland formation, mucin production, and/or desmoplastic or fibrotic reaction, were not obvious in mice with a *Sav1*$^{+/-}$ or *Rassf1a*$^{-/-}$ genotype although most of the livers from *Sav1*$^{+/-}$ mice showed signs of oval cell expansion or bile duct hyperplasia (Fig. 2E,F).

Analysis of the Hippo pathway

Conditional biallelic deletion of the *Sav1* gene in the mouse liver induces liver enlargement and liver tumor formation (17,18). Although in our work close to 100% of *Rassf1a*$^{+/+}$ *Sav1*$^{+/-}$ mice or *Rassf1a*$^{-/-}$ *Sav1*$^{+/-}$ mice developed liver tumors after 12 months of age, we did not find any liver enlargement before tumors developed (Fig. S4). This finding suggests that one copy of *Sav1* is sufficient to prevent liver enlargement but is insufficient to prevent liver tumor formation. Complete loss of *Rassf1a* does not lead to liver enlargement either (Fig. S4).

Since SAV1 and RASSF1A are components and potential regulators of the Hippo pathway, we analyzed levels of MST1 and MST2, YAP protein levels and phosphorylation on serine 127 of YAP in normal-appearing livers of mice of the different genotypes at the age of 6 months (Fig. 3A). If the Hippo pathway is dysfunctional in gene-targeted mice, YAP protein should be less phosphorylated and total levels of YAP should increase owing to diminished degradation of YAP. First, we found that protein levels of both MST1 and MST2 were substantially reduced in the livers of *Rassf1a*$^{+/+}$ *Sav1*$^{+-}$ mice. In *Rassf1a*$^{-/-}$ *Sav1*$^{+/+}$ mice, MST1 was decreased in only one of three mice and MST2 levels were similar to those in wildtype mice. In the double knockout mice, levels of MST1 were strongly decreased but MST2 appeared at wildtype levels suggesting complex regulation of MST levels upon loss of their scaffold proteins (Fig. 3A).

However, levels of YAP and phosphorylated YAP, their ratio, or levels of the YAP homologue TAZ did not differ noticeably in livers of all the genotypes (Fig. 3A). This suggested that although levels of MST1/2 were affected by deletion of SAV1, the standard readouts of the Hippo pathway, YAP and p-YAP, appeared largely unaltered in non-tumorous liver. Comparing liver tumors developing in *Sav1*$^{+/-}$ mice with adjacent normal liver tissue, we found much reduced levels of SAV1 protein in the majority of the tumors (Fig. 3B). Increased transcript level of the YAP target gene *Ctgf* is a marker of a dysfunctional Hippo pathway (32). We determined the gene expression levels of *Ctgf* in liver tumors developing in *Rassf1a*$^{+/+}$ *Sav1*$^{+/-}$ mice. Thirteen of 14 liver tumor tissues expressed increased levels of *Ctgf* compared to the adjacent normal tissues (Fig. 3C). The high level of *Ctgf* expression in two tumors that retained SAV1 protein may be due to Hippo/YAP-independent mechanisms. We did not retain sufficient numbers of frozen tumors from *Rassf1a*$^{-/-}$ *Sav1*$^{+/+}$ mice to compare *Ctgf* levels. The data suggests that the remaining *Sav1* copy or perhaps other components of the pathway in the livers of *Sav1*$^{+/-}$ mice may eventually become disabled in founder cells giving rise to a dysfunctional Hippo pathway and producing liver tumors. However, the overall protein expression levels of YAP and phosphorylated YAP are not noticeably altered in bulk liver tissue of *Sav1* heterozygous or *Rassf1a* homozygous mutant mice (Fig. 3A).

TBK1, a new RASSF1A-interacting protein

To identify potentially novel RASSF1A-interacting proteins, we performed immunoprecipitation of endogenous RASSF1A from HeLa cells. Co-precipitating proteins were identified by mass spectrometry (Fig. 4A). The most significantly enriched proteins were three kinases, MST1, MST2 and TBK1 (Tank binding kinase 1). Figure 4B shows co-

immunoprecipitation of endogenous RASSF1A and TBK1. TBK1 is an oncogenic noncanonical IkB kinase, which phosphorylates IkB to release NFkB, which can induce the transcription of various pro-inflammatory and anti-apoptotic genes (33,34). We then analyzed protein expression levels of TBK1 in *Rassf1a*$^{-/-}$ *Sav1*$^{+/+}$ mouse liver tissues and found that TBK1 protein expression was consistently and substantially increased in all *Rassf1a* knockout livers compared with the wild type livers at the same age (18 months) (Fig. 4C). A similar increase of TBK1 levels was consistently found at earlier and later ages of the mice and also was seen in *Rassf1a*$^{-/-}$ *Sav1*$^{+/-}$ double knockout mice but not in *Rassf1a*$^{+/+}$ *Sav1*$^{+/-}$ mice (data not shown).

The best-studied functions of TBK1 are through regulating the classical NFkB pathway via p65 phosphorylation. Therefore, we determined the total protein expression of p65, its phosphorylated form p-p65 and its binding partner, NFkB1/p50 which complexes with p65 and IkBα in the cytoplasm. p65 or p-p65 did not show a notable increase in *Rassf1a*$^{-/-}$ *Sav1*$^{+/+}$ mice. Also, p105 and its truncated form p50 did not consistently show higher protein levels upon *Rassf1a* deletion (Fig. 4C).

The liver transcriptomes of Sav1 and Rassf1a knockout mice

We isolated RNA from livers of the four mouse genotypes at one year of age processing four biological replicates for each genotype. The RNA was analyzed on Affymetrix 1.0-ST microarrays. The four genotypes could be well separated by heat maps (Fig. 5A). Using a P-value cutoff of $P<0.005$, we found a relatively small number of up- or downregulated genes in *Rassf1a*$^{+/+}$ *Sav1*$^{+/-}$ mice relative to wildtype mice (Fig. 5B; Supplementary Tables S1 and S2). As expected, levels of *Sav1* transcripts were reduced to about 50%. However, at the same significance level, the transcriptomes of *Rassf1a*$^{-/-}$ *Sav1*$^{+/+}$ and *Rassf1a*$^{-/-}$ *Sav1*$^{+/-}$ mice were more substantially altered in comparison to those of *Rassf1a*$^{+/+}$ *Sav1*$^{+/-}$ mice (Fig. 5B; Tables S1 and S2). There was some overlap between the genotypes. Most notably, expression differences in both directions of *Rassf1a*$^{-/-}$ *Sav1*$^{+/+}$ and *Rassf1a*$^{-/-}$ *Sav1*$^{+/-}$ mice relative to wildtype were more similar to each other than to *Rassf1a*$^{+/+}$ *Sav1*$^{+/-}$ mice (Fig. 5B; Table S2).

Gene ontology analysis did not provide any enrichment for specific gene or functional categories in the *Rassf1a*$^{+/+}$ *Sav1*$^{+/-}$ mice. In contrast, the same analysis for the *Rassf1a*-deleted genotypes uncovered enrichment of two major functional categories: the circadian clock and microtubule polymerization (Fig. S5). This analysis did not reveal a gene category related to the NFkB pathway or to inflammatory responses in *Rassf1a*$^{-/-}$ genotype livers that could perhaps be traced back to increased levels of TBK1. Interestingly, however, we found that several beta tubulin genes, including *Tubb1*, *Tubb2a*, *Tubb2b* and *Tubb5* were among the top 60 upregulated genes in *Rassf1a* knockout livers (Supplementary Table S1). These beta tubulin genes were significantly upregulated (up to 4-fold) in *Rassf1a*$^{-/-}$ *Sav1*$^{+/+}$ and *Rassf1a*$^{-/-}$ *Sav1*$^{+/-}$ mice but not in *Rassf1a*$^{+/+}$ *Sav1*$^{+/-}$ livers (Fig. 5C and Table S1). In fact, most beta tubulin genes were upregulated except for *Tubb3* and *Tubb4a*, which are beta tubulin isoforms preferentially expressed in the nervous system. Genes coding for alpha and gamma tubulin proteins were not significantly different in the knockouts. At the protein level, TUBB2A was increased only slightly in livers of *Rassf1a* knockout mice (Fig. 5C).

The enrichment of circadian factors in *Rassf1a*-deleted livers (Fig. S5) was unexpected. One differentially expressed gene was *Usp2*. The ubiquitin-specific protease USP2 is a key driver of the circadian clock (35). Interestingly, USP2 is also a binding partner and negative regulator of the Rassf1a interacting kinase, TBK1 (36). Although *Tbk1* itself was not transcriptionally misregulated in *Rassf1a* knockout mice, we observed that at the transcript level, factors regulating TBK1 protein stability, including *Usp2* and *Dtx4*, were dysregulated. *Usp2* was the second most significantly altered gene in *Rassf1a*$^{-/-}$ *Sav1*$^{+/+}$ livers (downregulated ~16-fold; Table S1). *Dtx4*, the sixth most significantly altered (upregulated) gene (Table S1) in this genotype is an E3 ubiquitin ligase and key suppressor of TBK1 targeting this kinase for degradation (37). The data suggest that a regulatory feedback loop may exist between RASSF1A, TBK1 and its modifiers DTX4 and USP2.

Human liver cancers show frequent methylation of the RASSF1A promoter, but minimal methylation of other Hippo pathway genes

Promoter hypermethylation of tumor suppressor genes is a potential contributor to tumor formation. Since mutations in genes of the Hippo pathway are uncommon in human cancers (16) including liver cancer, we analyzed several genes of the pathway for methylation at their promoters in 22 pairs of human normal tissue and tumor tissue of the liver (Fig. S6, S7; Table S3). Liver cancer patients often have predisposing conditions including cirrhosis, HBV, or HCV (Table S3). We analyzed promoter methylation of the target genes by using combined bisulfite restriction analysis (COBRA) on normal tissues and tumor tissues (Fig. S6, S7). Seventeen out of 22 (77%) of the liver cancer patients had higher *RASSF1A* methylation in the tumor tissues compared with the adjacent normal tissues (Fig. S6A). Partial methylation of *RASSF1A* was seen in some tumor-adjacent livers and in liver DNA from an 83-year old tumor-free liver. Our RASSF1A promoter methylation data are consistent with other groups' earlier findings showing extensive methylation of *RASSF1A* in HCC (38-40). However, we detected no methylation at the *SAV1* promoter (Fig. S6B). Furthermore, we found no methylation in human liver tumors at the promoters of the genes *MST1* and *MST2* (Fig. S7).

To support this analysis, we analyzed HCC DNA methylation data from TCGA (Fig. 6). This analysis shows methylation of the *RASSF1A* but not the *RASSF1C* or *SAV1* promoters in HCC in the TCGA data set. The more highly methylated tumors (indicated by a dotted line in Fig. 6A) had the lowest expression of *RASSF1A*. Although the TCGA sample number for normal liver is still limited, there seems to be a trend for lower expression of *SAV1* in some HCCs. However, about half of the HCCs still express high levels of *SAV1* (Fig. 6B). Analysis of TCGA data for *MST1* and *MST2* also show a lack of methylation at their promoter-associated CpG islands (Fig. S8). *MST1* is expressed at rather high levels and is downregulated in very few HCCs. Unexpectedly, *MST2* is upregulated in about half the HCCs relative to normal liver tissues (Fig. S8B). This data suggests that the *RASSF1A* gene is frequently and extensively methylated and silenced in human liver tumors but that *SAV1* or *MST1/2* are less commonly affected.

Discussion

In this study, we created three mouse models in which scaffold protein binding partners of the mammalian Hippo kinases MST1 and MST2 were deleted. Liver-specific deletion of *Mst1* and *Mst2* together (18-20), as well as liver-specific homozygous deletion of *Sav1* (17,18), produced hepatomegaly and effectively induced hepatocellular carcinomas in mice. These deletions increase the pool of hepatic progenitor cells (oval cells), a phenomenon we also observed in our $Sav1^{+/-}$ mice and to a lesser extent in $Rassf1a^{-/-}$ mice. $Sav1^{+/-}$ mice also developed liver cancer in a previous study (17). It remains unknown why constitutive deletion of *Sav1* in the mouse has such a prominent effect on liver tumor formation and rarely affects other tissues even though YAP, its best-studied downstream effector, plays a general role in many cell types.

In our comparative mouse studies, we determined that homozygous deletion of *Rassf1a* causes liver tumor susceptibility. In previous studies, liver tumors were not observed as a common type of tumor in $Rassf1a^{-/-}$ mice (4,5). These mice were on a different genetic background (129SvJ x C57BL/6). The heterozygous deletion of *Sav1* was much more potent in promoting liver cancer (Table 1) even though both RASSF1A and SAV1 are binding partners and activators of the MST kinases (10,14,41). Although we are unable to offer a definitive explanation for these differences in tumor susceptibility between the *Sav1* and *Rassf1a* deleted genotypes at this time, one likely possibility is the redundancy of the RASSF protein family. While there is only one SAV1-like protein in mammalian genomes, there are 10 RASSF proteins defined by the presence of a RAS association domain (42). Six of these proteins (RASSF1-6) have a C-terminal RAS association domain. The proteins most closely related to RASSF1 are RASSF3 and RASSF5 (a.k.a. NORE1). We found that the *Rassf5* gene was upregulated 1.24-fold in the liver of *Rassf1a* knockout mice (Table S1) but other *Rassf* genes were not changed. Deletion of multiple members of the C-terminal *Rassf* family may be necessary to elicit a more dramatic phenotype in animal models.

Mice with heterozygous deletion of *Sav1* or homozygous deletion of *Rassf1a* did not show any signs of liver enlargement prior to development of tumors in contrast to mice with conditional ablation of *Sav1* or *Mst1* and *Mst2* in the liver (17-20) or liver-specific overexpression of *Yap* (43). This data suggests that the core Hippo pathway restraining tissue overgrowth by inhibiting YAP activity in the liver is functional in the absence of *Rassf1a* or in presence of only one copy of *Sav1*. However, these deletions led to the formation of liver tumors. It is likely that the remaining functional copy of *Sav1* is lost or disabled in tumor-initiating cells of $Sav1^{+/-}$ livers. The downstream consequences are activation of YAP-dependent expression of pro-growth genes as exemplified by increased expression of *Ctgf* (Fig. 3C). The phenotype of *Rassf1a* homozygous deletion is milder than that of *Sav1* single copy deletion but is still pronounced. It can be hypothesized that loss of *Rassf1a* cooperates with other tumor-driving events in liver cancer formation as previously demonstrated for hematological malignancies (6).

Besides its involvement in the Hippo pathway, RASSF1A has additional functions that when impaired may contribute to malignant transformation. As an established microtubule binding and stabilizing protein (8), loss of RASSF1A may interfere with events such as cell

migration (44) and mitosis (8,10,45,46). Defects in cell migration or mitosis are likely contributors to oncogenesis. Interestingly, we observed that loss of *Rassf1a* leads to increased expression of a number of beta tubulin isoform-encoding genes including *Tubb1*, *Tubb2a*, *Tubb2b* and *Tubb5*. This finding suggests that loss of microtubule stabilization by RASSF1A may invoke compensatory events by increasing transcription of beta tubulin genes. However, this compensation may be insufficient contributing to the tumor-promoting phenotype of *Rassf1a* loss.

We identified the kinase TBK1 as a strong RASSF1A-interacting protein (Fig. 4). This interaction was further proven to be relevant in vivo by the clearly enhanced levels of TBK1 protein in every liver sample obtained from mice with *Rassf1a* deletion. The absence of a protein commonly leads to diminished levels of its binding partner(s) owing to reduced protein stability in absence of the partner. However, this is not the case with TBK1, which showed increased levels upon deletion of *Rassf1a*. One possible explanation is that RASSF1A promotes degradation of TBK1 upon binding, a scenario, which requires additional investigation. In any event, the data suggest that RASSF1A is a negative regulator of the oncogenic kinase TBK1 because in the absence of RASSF1A, the levels of this kinase are increased. TBK1 is best known as an activator of the NFkB pathway and has oncogenic properties (33,34). Deletion of *Rassf1a* did not lead to a noticeable activation of the pathway and of NFkB target genes in the liver (Fig. 4; Table S1). We also did not observe an increase of inflammatory cells in sections of livers from *Rassf1a*$^{-/-}$ mice. For these reasons, NFkB pathway-independent functions of TBK1 may be important for tumor promotion in the liver and these may be increased upon loss of *Rassf1a*. Mouse models have shown that TBK1 is critical in protecting the liver from apoptosis (47). TBK1 can directly activate AKT by phosphorylating the activation loop (48). Furthermore, it has been shown that TBK1 is a mitotic kinase that phosphorylates and activates Polo-like kinase 1 (PLK1) (49). Interference with mitotic progression is generally a potential tumor-promoting event. Importantly, a role of RASSF1A and the Hippo pathway in mitotic exit and prevention of polyploidy has been proposed previously (10), suggesting that loss of RASSF1A may have a multipronged effect on correct execution of mitosis, which may explain aspects of the tumor-predisposing phenotype of *Rassf1a* loss.

Lastly, our studies add information to the possible role of the Hippo pathway in human liver cancer. Several mouse models with deletions of core components of the pathway clearly suggest that failure of Hippo signaling promotes liver cancer (50). However, mutations of *SAV1*, *RASSF1A*, *MST1*, *MST2*, or *LATS1*, *LATS2* are extremely rare in human cancer (16). Although upstream Hippo signaling regulators such as *FAT1*, *FAT4*, or *NF2* may be mutated in certain types of malignancies, they are not commonly mutated in human liver cancer either. Therefore, one may consider epigenetic inactivation of Hippo pathway tumor suppressor genes as a potential tumor-driving event. However, our own studies (Fig. S6, S7) along with previous data (38-40) and data obtained from TCGA (Fig. 6; Fig. S8) suggest that the only Hippo pathway gene commonly silenced by epigenetic processes in HCC is *RASSF1A*. This is particularly puzzling inasmuch as epigenetic inactivation of *SAV1* would be expected to be a much more efficient tumor-promoting event than silencing of *RASSF1A*, given the data from our mouse models. Although *SAV1* seems to be downregulated in a subset of HCCs, *MST2* is overexpressed rather than downregulated in many of the TCGA

samples. Furthermore, although *Sav1* mutant livers are characterized by an expansion of the oval cell pool, recent data has cast doubt onto whether these progenitor cells can be considered general precursors of HCC in various liver cancer models, as opposed to mature hepatocytes which may undergo dedifferentiation (51). Future studies are needed to resolve the complex roles of the Hippo pathway in human HCC.

Supplementary Material

Refer to Web version on PubMed Central for supplementary material.

Acknowledgments

Financial Support:

This work was supported by a grant of the University of California Tobacco-Related Disease Research Program (17RT-0116) and by NIH grant CA084469 to GPP.

References

1. Dammann R, Li C, Yoon JH, Chin PL, Bates S, Pfeifer GP. Epigenetic inactivation of a RAS association domain family protein from the lung tumour suppressor locus 3p21.3. Nat Genet. 2000; 25(3):315–9. [PubMed: 10888881]
2. Agathanggelou A, Cooper WN, Latif F. Role of the Ras-association domain family 1 tumor suppressor gene in human cancers. Cancer Res. 2005; 65(9):3497–508. [PubMed: 15867337]
3. Grawenda AM, O'Neill E. Clinical utility of RASSF1A methylation in human malignancies. Br J Cancer. 2015; 113(3):372–81. [PubMed: 26158424]
4. Tommasi S, Dammann R, Zhang Z, Wang Y, Liu L, Tsark WM, et al. Tumor susceptibility of Rassf1a knockout mice. Cancer Res. 2005; 65(1):92–8. [PubMed: 15665283]
5. van der Weyden L, Tachibana KK, Gonzalez MA, Adams DJ, Ng BL, Petty R, et al. The RASSF1A isoform of RASSF1 promotes microtubule stability and suppresses tumorigenesis. Mol Cell Biol. 2005; 25(18):8356–67. [PubMed: 16135822]
6. van der Weyden L, Papaspyropoulos A, Poulogiannis G, Rust AG, Rashid M, Adams DJ, et al. Loss of RASSF1A synergizes with deregulated RUNX2 signaling in tumorigenesis. Cancer Res. 2012; 72(15):3817–27. [PubMed: 22710434]
7. Ortiz-Vega S, Khokhlatchev A, Nedwidek M, Zhang XF, Dammann R, Pfeifer GP, et al. The putative tumor suppressor RASSF1A homodimerizes and heterodimerizes with the Ras-GTP binding protein Nore1. Oncogene. 2002; 21(9):1381–90. [PubMed: 11857081]
8. Liu L, Tommasi S, Lee DH, Dammann R, Pfeifer GP. Control of microtubule stability by the RASSF1A tumor suppressor. Oncogene. 2003; 22(50):8125–36. [PubMed: 14603253]
9. El-Kalla M, Onyskiw C, Baksh S. Functional importance of RASSF1A microtubule localization and polymorphisms. Oncogene. 2010; 29(42):5729–40. [PubMed: 20697344]
10. Guo C, Tommasi S, Liu L, Yee JK, Dammann R, Pfeifer GP. RASSF1A is part of a complex similar to the Drosophila Hippo/Salvador/Lats tumor-suppressor network. Curr Biol. 2007; 17(8): 700–5. [PubMed: 17379520]
11. Khokhlatchev A, Rabizadeh S, Xavier R, Nedwidek M, Chen T, Zhang XF, et al. Identification of a novel Ras-regulated proapoptotic pathway. Curr Biol. 2002; 12(4):253–65. [PubMed: 11864565]
12. Guo C, Zhang X, Pfeifer GP. The tumor suppressor RASSF1A prevents dephosphorylation of the mammalian STE20-like kinases MST1 and MST2. J Biol Chem. 2011; 286(8):6253–61. [PubMed: 21199877]
13. Tapon N, Harvey KF, Bell DW, Wahrer DC, Schiripo TA, Haber D, et al. salvador Promotes both cell cycle exit and apoptosis in Drosophila and is mutated in human cancer cell lines. Cell. 2002; 110(4):467–78. [PubMed: 12202036]

14. Harvey K, Tapon N. The Salvador-Warts-Hippo pathway - an emerging tumour- suppressor network. Nat Rev Cancer. 2007; 7(3):182–91. [PubMed: 17318211]
15. Huang J, Wu S, Barrera J, Matthews K, Pan D. The Hippo signaling pathway coordinately regulates cell proliferation and apoptosis by inactivating Yorkie, the Drosophila Homolog of YAP. Cell. 2005; 122(3):421–34. [PubMed: 16096061]
16. Harvey KF, Zhang X, Thomas DM. The Hippo pathway and human cancer. Nat Rev Cancer. 2013; 13(4):246–57. [PubMed: 23467301]
17. Lee KP, Lee JH, Kim TS, Kim TH, Park HD, Byun JS, et al. The Hippo-Salvador pathway restrains hepatic oval cell proliferation, liver size, and liver tumorigenesis. Proc Natl Acad Sci USA. 2010; 107(18):8248–53. [PubMed: 20404163]
18. Lu L, Li Y, Kim SM, Bossuyt W, Liu P, Qiu Q, et al. Hippo signaling is a potent in vivo growth and tumor suppressor pathway in the mammalian liver. Proc Natl Acad Sci USA. 2010; 107(4):1437–42. [PubMed: 20080689]
19. Zhou D, Conrad C, Xia F, Park JS, Payer B, Yin Y, et al. Mst1 and Mst2 maintain hepatocyte quiescence and suppress hepatocellular carcinoma development through inactivation of the Yap1 oncogene. Cancer cell. 2009; 16(5):425–38. [PubMed: 19878874]
20. Song H, Mak KK, Topol L, Yun K, Hu J, Garrett L, et al. Mammalian Mst1 and Mst2 kinases play essential roles in organ size control and tumor suppression. Proc Natl Acad Sci USA. 2010; 107(4):1431–6. [PubMed: 20080598]
21. Fujimoto A, Furuta M, Shiraishi Y, Gotoh K, Kawakami Y, Arihiro K, et al. Whole-genome mutational landscape of liver cancers displaying biliary phenotype reveals hepatitis impact and molecular diversity. Nat Commun. 2015; 6:6120. [PubMed: 25636086]
22. Schulze K, Imbeaud S, Letouze E, Alexandrov LB, Calderaro J, Rebouissou S, et al. Exome sequencing of hepatocellular carcinomas identifies new mutational signatures and potential therapeutic targets. Nat Genet. 2015; 47(5):505–11. [PubMed: 25822088]
23. Huang J, Deng Q, Wang Q, Li KY, Dai JH, Li N, et al. Exome sequencing of hepatitis B virus-associated hepatocellular carcinoma. Nat Genet. 2012; 44(10):1117–21. [PubMed: 22922871]
24. Zhao B, Wei X, Li W, Udan RS, Yang Q, Kim J, et al. Inactivation of YAP oncoprotein by the Hippo pathway is involved in cell contact inhibition and tissue growth control. Genes Dev. 2007; 21(21):2747–61. [PubMed: 17974916]
25. Zender L, Spector MS, Xue W, Flemming P, Cordon-Cardo C, Silke J, et al. Identification and validation of oncogenes in liver cancer using an integrative oncogenomic approach. Cell. 2006; 125(7):1253–67. [PubMed: 16814713]
26. Lee JH, Kim TS, Yang TH, Koo BK, Oh SP, Lee KP, et al. A crucial role of WW45 in developing epithelial tissues in the mouse. EMBO J. 2008; 27(8):1231–42. [PubMed: 18369314]
27. Tang SH, Silva FJ, Tsark WM, Mann JR. A Cre/loxP-deleter transgenic line in mouse strain 129S1/SvImJ. Genesis. 2002; 32(3):199–202. [PubMed: 11892008]
28. Dimauro I, Pearson T, Caporossi D, Jackson MJ. A simple protocol for the subcellular fractionation of skeletal muscle cells and tissue. BMC Res Notes. 2012; 5:513. [PubMed: 22994964]
29. Xiong Z, Laird PW. COBRA: a sensitive and quantitative DNA methylation assay. Nucleic Acids Res. 1997; 25(12):2532–4. [PubMed: 9171110]
30. Schagdarsurengin U, Richter AM, Hornung J, Lange C, Steinmann K, Dammann RH. Frequent epigenetic inactivation of RASSF2 in thyroid cancer and functional consequences. Mol Cancer. 2010; 9:264. [PubMed: 20920251]
31. Thoolen B, Maronpot RR, Harada T, Nyska A, Rousseaux C, Nolte T, et al. Proliferative and nonproliferative lesions of the rat and mouse hepatobiliary system. Toxicol Pathol. 2010; 38(7 Suppl):5S–81S. [PubMed: 21191096]
32. Zhao B, Ye X, Yu J, Li L, Li W, Li S, et al. TEAD mediates YAP-dependent gene induction and growth control. Genes Dev. 2008; 22(14):1962–71. [PubMed: 18579750]
33. Barbie DA, Tamayo P, Boehm JS, Kim SY, Moody SE, Dunn IF, et al. Systematic RNA interference reveals that oncogenic KRAS-driven cancers require TBK1. Nature. 2009; 462(7269): 108–12. [PubMed: 19847166]

34. Chien Y, Kim S, Bumeister R, Loo YM, Kwon SW, Johnson CL, et al. RalB GTPase-mediated activation of the IkappaB family kinase TBK1 couples innate immune signaling to tumor cell survival. Cell. 2006; 127(1):157–70. [PubMed: 17018283]
35. Scoma HD, Humby M, Yadav G, Zhang Q, Fogerty J, Besharse JC. The de ubiquitinylating enzyme, USP2, is associated with the circadian clockwork and regulates its sensitivity to light. PloS one. 2011; 6(9):e25382. [PubMed: 21966515]
36. Zhang L, Zhao X, Zhang M, Zhao W, Gao C. Ubiquitin-specific protease 2b negatively regulates IFN-beta production and antiviral activity by targeting TANK-binding kinase 1. J Immunol. 2014; 193(5):2230–7. [PubMed: 25070846]
37. Cui J, Li Y, Zhu L, Liu D, Songyang Z, Wang HY, et al. NLRP4 negatively regulates type I interferon signaling by targeting the kinase TBK1 for degradation via the ubiquitin ligase DTX4. Nat Immunol. 2012; 13(4):387–95. [PubMed: 22388039]
38. Schagdarsurengin U, Wilkens L, Steinemann D, Flemming P, Kreipe HH, Pfeifer GP, et al. Frequent epigenetic inactivation of the RASSF1A gene in hepatocellular carcinoma. Oncogene. 2003; 22(12):1866–71. [PubMed: 12660822]
39. Zhang YJ, Ahsan H, Chen Y, Lunn RM, Wang LY, Chen SY, et al. High frequency of promoter hypermethylation of RASSF1A and p16 and its relationship to aflatoxin B1-DNA adduct levels in human hepatocellular carcinoma. Mol Carcinog. 2002; 35(2):85–92. [PubMed: 12325038]
40. Zhong S, Yeo W, Tang MW, Wong N, Lai PB, Johnson PJ. Intensive hypermethylation of the CpG island of Ras association domain family 1A in hepatitis B virus-associated hepatocellular carcinomas. Clin Cancer Res. 2003; 9(9):3376–82. [PubMed: 12960125]
41. Udan RS, Kango-Singh M, Nolo R, Tao C, Halder G. Hippo promotes proliferation arrest and apoptosis in the Salvador/Warts pathway. Nat Cell Biol. 2003; 5(10):914–20. [PubMed: 14502294]
42. Pfeifer GP, Dammann R, Tommasi S. RASSF proteins. Curr Biol. 2010; 20(8):R344–R45. [PubMed: 21749948]
43. Dong J, Feldmann G, Huang J, Wu S, Zhang N, Comerford SA, et al. Elucidation of a universal size-control mechanism in Drosophila and mammals. Cell. 2007; 130(6):1120–33. [PubMed: 17889654]
44. Dallol A, Agathanggelou A, Tommasi S, Pfeifer GP, Maher ER, Latif F. Involvement of the RASSF1A tumor suppressor gene in controlling cell migration. Cancer Res. 2005; 65(17):7653–9. [PubMed: 16140931]
45. Dallol A, Agathanggelou A, Fenton SL, Ahmed-Choudhury J, Hesson L, Vos MD, et al. RASSF1A interacts with microtubule-associated proteins and modulates microtubule dynamics. Cancer Res. 2004; 64(12):4112–6. [PubMed: 15205320]
46. Vos MD, Martinez A, Elam C, Dallol A, Taylor BJ, Latif F, et al. A role for the RASSF1A tumor suppressor in the regulation of tubulin polymerization and genomic stability. Cancer Res. 2004; 64(12):4244–50. [PubMed: 15205337]
47. Bonnard M, Mirtsos C, Suzuki S, Graham K, Huang J, Ng M, et al. Deficiency of T2K leads to apoptotic liver degeneration and impaired NF-kappaB-dependent gene transcription. EMBO J. 2000; 19(18):4976–85. [PubMed: 10990461]
48. Ou YH, Torres M, Ram R, Formstecher E, Roland C, Cheng T, et al. TBK1 directly engages Akt/PKB survival signaling to support oncogenic transformation. Mol Cell. 2011; 41(4):458–70. [PubMed: 21329883]
49. Kim JY, Welsh EA, Oguz U, Fang B, Bai Y, Kinose F, et al. Dissection of TBK1 signaling via phosphoproteomics in lung cancer cells. Proc Natl Acad Sci USA. 2013; 110(30):12414–9. [PubMed: 23836654]
50. Avruch J, Zhou D, Fitamant J, Bardeesy N. Mst1/2 signalling to Yap: gatekeeper for liver size and tumour development. Br J Cancer. 2011; 104(1):24–32. [PubMed: 21102585]
51. Font-Burgada J, Shalapour S, Ramaswamy S, Hsueh B, Rossell D, Umemura A, et al. Hybrid periportal hepatocytes regenerate the injured liver without giving rise to cancer. Cell. 2015; 162(4): 766–79. [PubMed: 26276631]

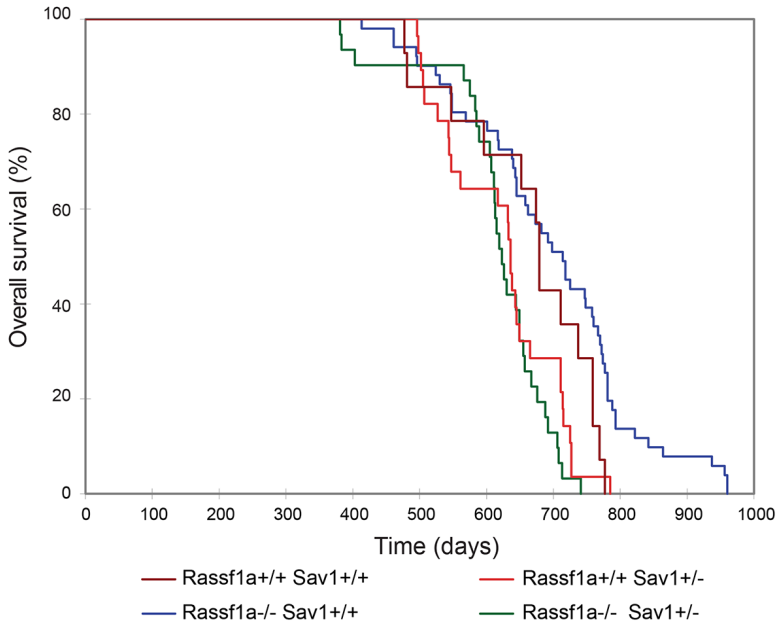

Figure 1. Survival of *Rassf1a* and *Sav1* knockout mice

Overall survival is plotted for *Rassf1a*$^{+/+}$ *Sav1*$^{+/+}$, *Rassf1a*$^{-/-}$ *Sav1*$^{+/+}$, *Rassf1a*$^{+/+}$ *Sav1*$^{+/-}$, and *Rassf1a*$^{-/-}$ *Sav1*$^{+/-}$ mice.

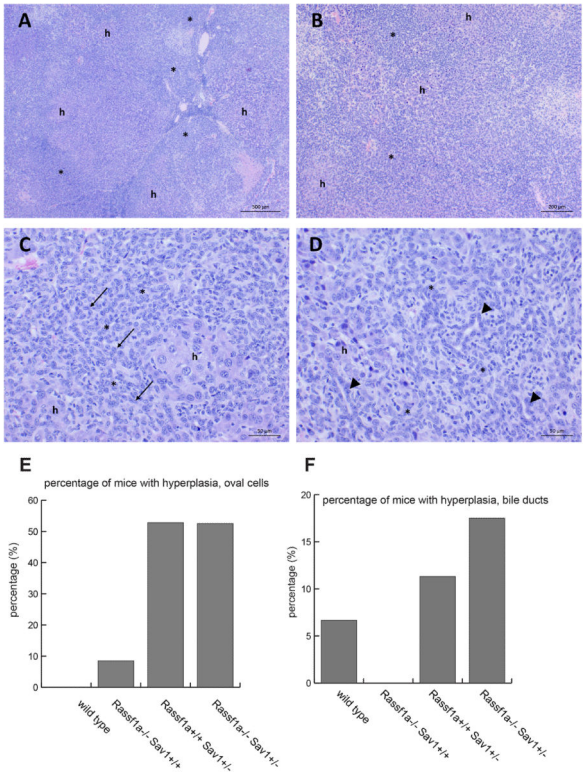

Figure 2. Characterization of liver tumors

A-D. Liver tumor from a *Sav1*$^{+/+}$ *Rassf1a*$^{-/-}$ mouse. Low magnification photomicrograph demonstrating multinodular "mixed" type tumor (panel A). Areas with obvious hepatocellular morphology (h) are intermixed with areas having "small cell" morphology (*). This is shown at slightly higher magnification in panel B. At still higher magnification (panels C and D), the "small cell" component (*) of the mixed tumors is found to be composed of cells that have oval to occasionally round or elongated nuclei (panel C; arrows) and vary from having no organization (panel C) to well-defined (panel D) orientation into rows or duct-like structures (panels D; arrowheads). Areas of obvious hepatocellular morphology are labeled (h) in panels C and D. H&E staining. **E.** Percentage of mice with oval cell hyperplasia of the liver. **F.** Percentage of mice with bile duct hyperplasia.

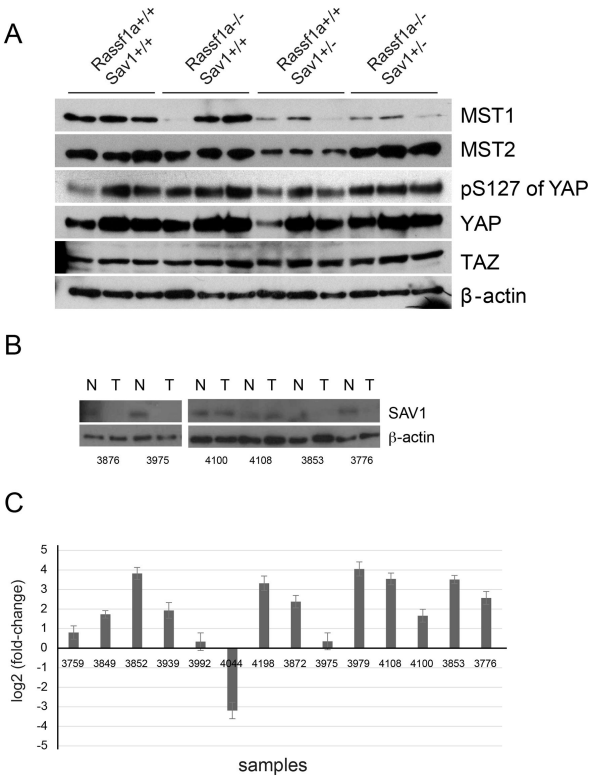

Figure 3. Analysis of Hippo pathway components

A. Western blot of Hippo pathway components in liver lysates of 6-month old mice of the different genotypes. Each lane represents a sample from an individual mouse. **B.** Reduction of SAV1 protein levels in liver tumors developing in *Rassf1a*$^{+/+}$ *Sav1*$^{+/-}$ mice. **C.** Expression differences of the YAP target gene *Ctgf* between liver tumors developing in *Rassf1a*$^{+/+}$ *Sav1*$^{+/-}$ mice and adjacent normal liver in the same mice. The expression data were normalized relative to *Gapdh* expression. All tumors were HCC except tumors 3852, 3872, 3939 and 3979, which were adenomas.

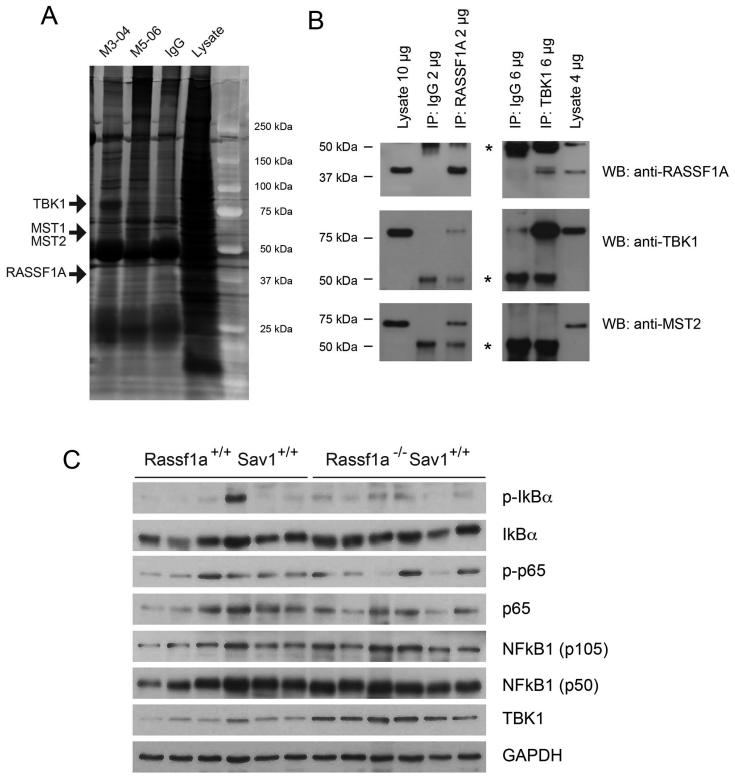

Figure 4. RASSF1A binds to and regulates the levels of the oncogenic kinase TBK1

A. Immunoprecipitation of RASSF1A-interacting proteins from HeLa cells. Endogenous RASSF1A was immunoprecipitated with two anti-RASSF1A antibodies, M3-04 and M5-06. Prominent bands on Coomassie blue stained gels were excised and proteins indicated by arrows were identified by mass spectrometry.

B. Proteins from HeLa cells were immunoprecipitated with anti-RASSF1A, anti-TBK1 antibodies or control IgG (IP). After separation on SDS gels, Western blots (WB) were conducted with the indicated antibodies. The asterisks indicate IgG bands.

C. Soluble cytosolic liver protein extracts from mice of different genotypes at 18 months of age were analyzed by Western blot for levels of TBK1 and proteins of the NFkB pathway. Each lane represents a sample from an individual mouse.

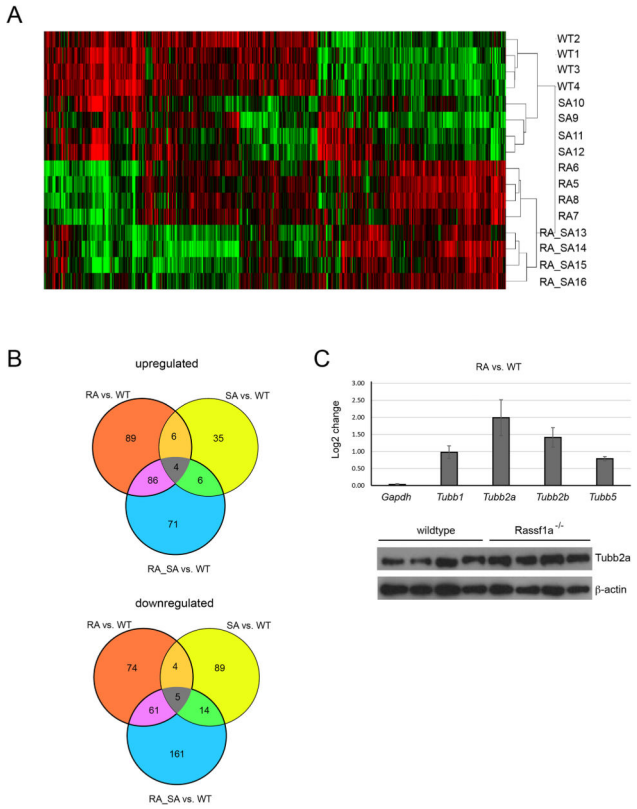

Figure 5. Gene expression differences in livers from mice with *Rassf1a* and/or *Sav1* deletion

A. Heat map showing differentially expressed genes in livers of 12-month old mice with genotypes $Rassf1a^{+/+}$ $Sav1^{+/+}$ (WT), $Rassf1a^{+/+}$ $Sav1^{+/-}$ (SA), $Rassf1a^{-/-}$ $Sav1^{+/+}$ (RA) and $Rassf1a^{-/-}$ $Sav1^{+/-}$ (RA_SA). Samples with the same genotype cluster together.

B. Venn diagram showing differentially expressed genes (P<=0.005), up- or downregulated, in the livers of the three knockout genotypes versus wildtype liver.

C. Differences in expression levels for the beta tubulin genes *Tubb1*, *Tubb2a, Tubb2b* and *Tubb5* as determined from the microarray data. Levels of TUBB2A protein in wildtype and $Rassf1a^{-/-}$ $Sav1^{+/+}$ mouse livers were assessed by Western blot using beta-actin as a control. Each lane represents a sample from an individual mouse.

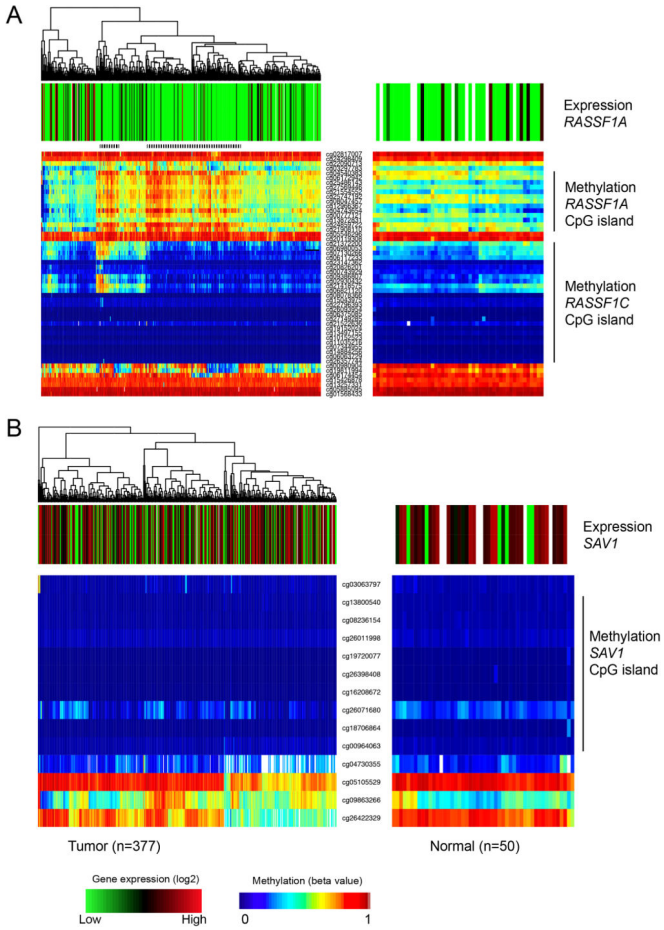

Figure 6. Methylation and expression of *RASSF1A* and *SAV1* in human HCC

A. Data for the *RASSF1* locus were extracted from TCGA data portal (http://cancergenome.nih.gov/). Expression (RNA-seq) and DNA methylation (Illumina 450k array) data were displayed for individual specimens (each column). The methylation data are plotted for individual CpG sites along the locus (each row). The dotted bar above the methylation data indicates groups of HCC specimens with higher level of DNA methylation at the *RASSF1A* CpG island that also show lack of gene expression (green). White bars show samples lacking expression data. **B.** TCGA data for the *SAV1* locus.

Table 1

Liver tumor formation in Rassf1a and Sav1 deficient mice

Rassf1a	Sav1	No. of Mice	Mean Age (days)	Median Age (days)	No of mice with hepatocellular tumors	Hepatocellular CA	Hepatocellular CA, mixed*	Hepatoblastoma	Hepatocellular adenoma	Hepatocellular adenoma, mixed*
wt	+/−	49	591	607	47 95.90%	35 71.40%	14 28.60%	0%	32 65.30%	17 34.70%
−/−	+/−	39	583	626	35 89.70%	30 77%	9 23.10%	1 2.60%	31 79.50%	15 38.50%
−/−	wt	45	643	642	19 42%	4 8.90%	1 2.20%	0 0%	14 31.10%	2 4.40%
wt	wt	30	613	659	6 20%	0 0%	0 0%	0 0%	6 20%	0 0%

*The designation mixed tumor refers to tumors which in addition to a hepatocellular component also had a “small cell / oval cell” component. Mean age and median age refer to overall survival of all mice of the respective genotype.